Cell Reports, Volume *26*

Supplemental Information

Dorsal Raphe Dual Serotonin-Glutamate Neurons Drive Reward by Establishing Excitatory Synapses on VTA Mesoaccumbens Dopamine Neurons

Hui-Ling Wang, Shiliang Zhang, Jia Qi, Huikun Wang, Roger Cachope, Carlos A. Mejias-Aponte, Jorge A. Gomez, Gabriel E. Mateo-Semidey, Gerard M.J. Beaudoin, Carlos A. Paladini, Joseph F. Cheer, and Marisela Morales

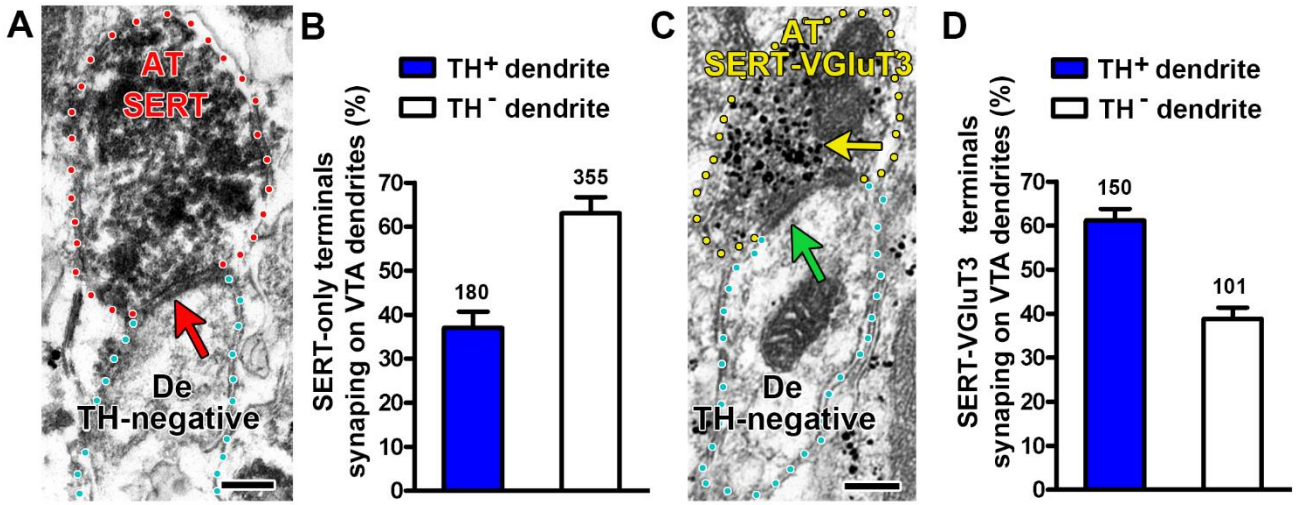

Figure S1. Both SERT-only and SERT-VGluT3 neurons synapse on VTA TH or non-TH neurons. Related to Figure 1.

A. SERT-only axon terminals (AT) make synapses on VTA TH-negative neurons, triple immunolabeling; TH label (gold particles); SERT-immunoperoxidase label (scattered dark material) and VGluT3 label (gold particles). SERT AT lacking VGluT3 (red outline) makes a symmetric synapse (red arrow) with a TH-negative dendrite (De, cyan outline). **B.** Frequency of SERT-only terminals synapsing on VTA dendrites. The bars represent mean + s.e.m. of the 2 classes of dendrites in the VTA of 4 mice from a total of 535 terminals (36.99 ± 3.72% SERT-only terminals on TH-positive dendrites and 63.01 ± 3.72% SERT-only terminals on TH-negative dendrites). $t_{(3)} = 3.498$, $P = 0.0395$, t-test. **C.** SERT-VGluT3 axon terminals (AT) make synapses on VTA TH-negative neurons, triple immunolabeling; TH label (gold particles); SERT-immunoperoxidase label (scattered dark material) and VGluT3 label (gold particles, yellow arrow). SERT-VGluT3 AT (yellow outline) makes an asymmetric synapse (green arrow) with a TH-negative dendrite (De, cyan outline). **D.** Frequency of SERT-VGluT3 terminals synapsing on VTA dendrites. The bars represent mean + s.e.m. of the 2 classes of dendrites in the VTA of 4 mice from a total of 251 terminals (61.17 ± 2.59% SERT-VGluT3 terminals on TH-positive dendrites and 38.83 ± 2.59% SERT-VGluT3 terminals on TH-negative dendrites). $t_{(3)} = 4.313$, $P = 0.0230$, t-test. Scale bars represent 200 nm in (A) and (C).

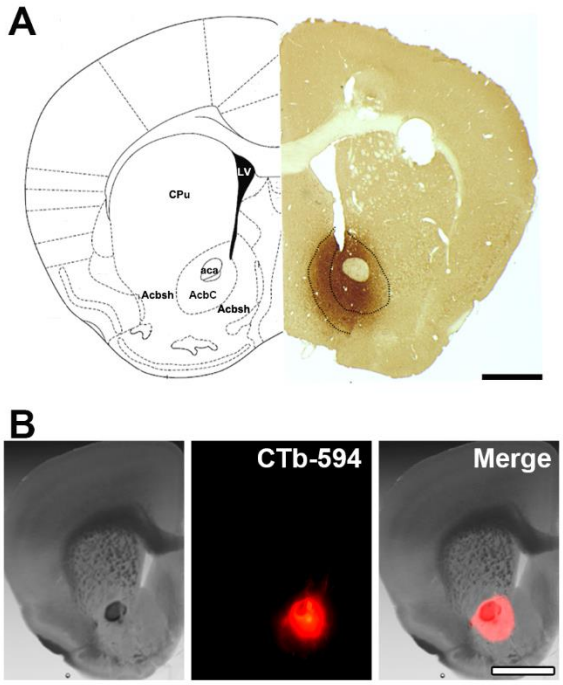

Figure S2. Histological verification of injection sites of FG or CTb in the nAcc of SERT::Cre mice. Related to Figure 2.

A. FG signal detected as brown material in the nAcc injection site. The diagram adapted from mouse atlas (bregma at 1.10mm). **B**. CTb signal detected as red fluorescence. aca, anterior commissure anterior part; AcbC, accumbens nucleus core; Acbsh, accumbens nucleus shell; CPu, caudate putamen; LV, lateral ventricle. Scale bars represent 1000 μm in (A) and 800 μm in (B).

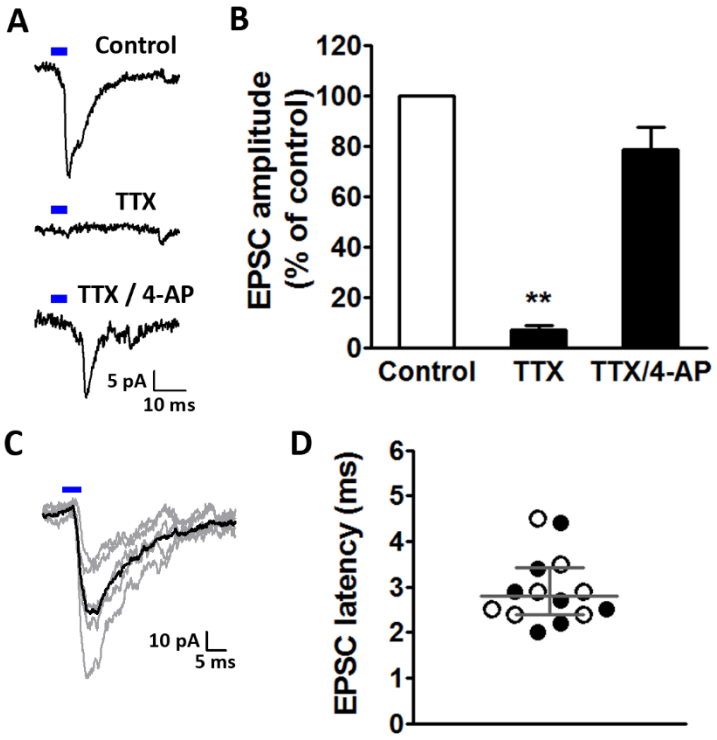

Figure S3. Monosynaptic glutamatergic transmission in DR-VTA pathway. Related to Figure 2.
A. Averaged traces show that optical-evoked EPSCs were eliminated by bath application of TTX (500 nM), and restored by application of 4-AP (200 μM). B. Summarized bar graph of the effects of TTX (6.9 ± 1.7% to control) and 4-AP (78.5 ± 9.1 % to control) on optical-evoked responses (n = 7; Repeated measures-ANOVA, F 2, 12 = 11.78, P = 0.001. ** P < 0.01 vs control, Newman-Keuls *post hoc* test). C. Sample traces of 5 consecutive recordings (gray) and the averaged response (black) showing short and consistent synaptic latency of the DR-VTA glutamatergic transmissions. Latency was defined as the time from the onset of laser pulses (blue line) to 10% of the peak responses. D. Summarized graph shows the averaged latency (2.94 ± 0.20 ms, n = 14) of the DR-VTA transmission. Black dots denote the monosynaptic latency of cells from the TTX/4-AP experiments (n = 7). Black circles denote the synaptic latency of cells from the CNQX experiments (n = 7; shown in Figure 2J), which are VTA mesoaccumbens DA neurons. Gray lines indicate the median and 25% and 75% quartiles of all cells.

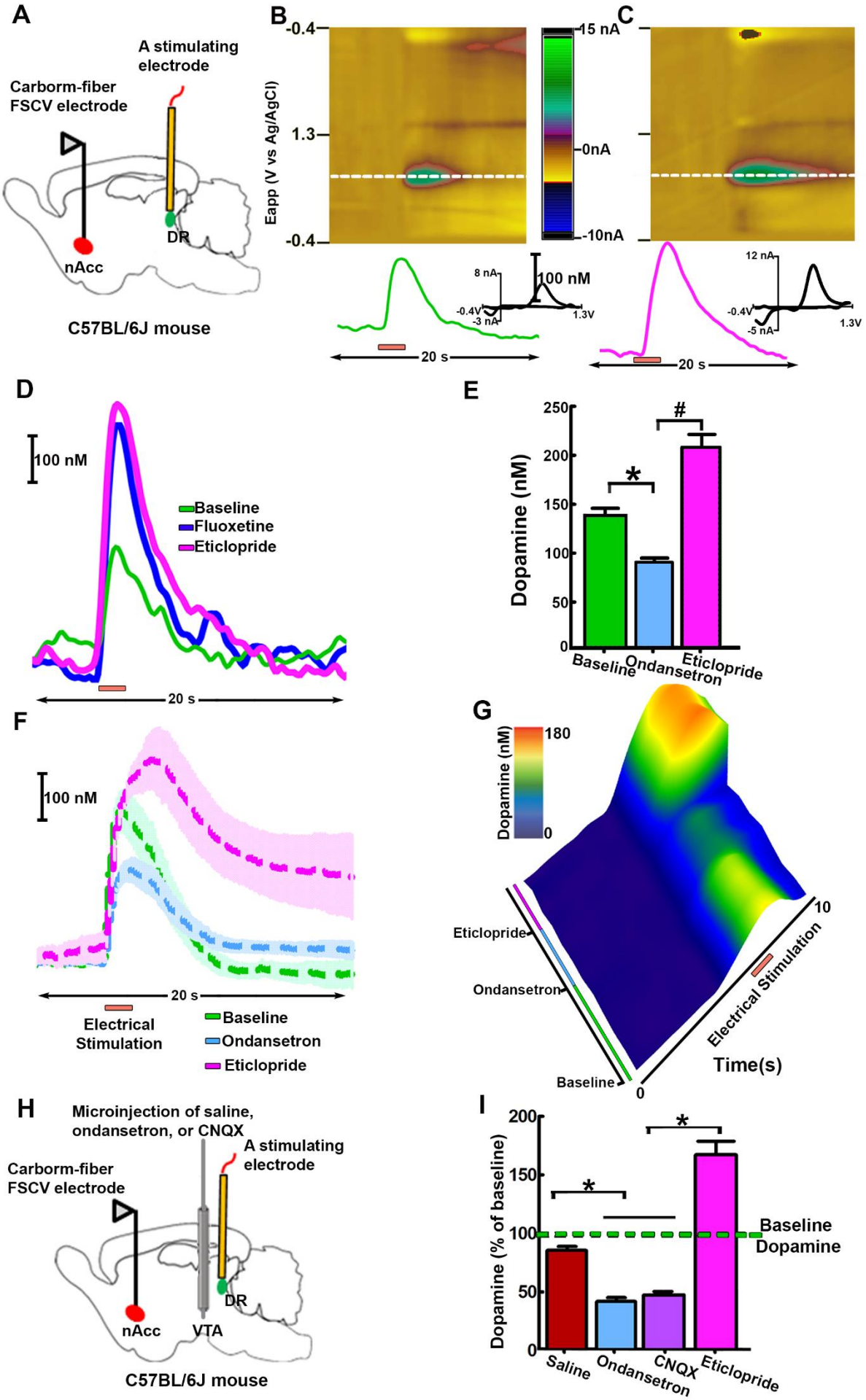
A
A stimulating electrode
Carborm-fiber FSCV electrode
DR
nAcc
C57BL/6J mouse
B
-0.4
1.3
-0.4
Eapp (V vs Ag/AgCl)
15 nA
0nA
-10nA
8 nA
-0.4V
-3 nA
100 nM
1.3V
20 s
C
12 nA
-0.4V
-5 nA
1.3V
20 s
D
100 nM
Baseline
Fluoxetine
Eticlopride
20 s
E
Dopamine (nM)
250
200
150
100
50
0
*
#
Baseline
Ondansetron
Eticlopride
F
100 nM
20 s
Electrical Stimulation
Baseline
Ondansetron
Eticlopride
G
Dopamine (nM)
180
0
Eticlopride
Ondansetron
Baseline
10
0
Electrical Stimulation
Time(s)
H
Microinjection of saline, ondansetron, or CNQX
A stimulating electrode
Carborm-fiber FSCV electrode
DR
nAcc
VTA
C57BL/6J mouse
I
Dopamine (% of baseline)
200
150
100
50
0
*
*
Baseline Dopamine
Saline
Ondansetron
CNQX
Eticlopride

Figure S4. Disrupting serotonin or glutamate signaling reduces dopamine release in the nAcc core evoked by DR electrical stimulation. Related to Figure 4.

A. Diagram showing electrical stimulation of DR neurons and measurement of dopamine release in the nAcc core by FSCV. **B.** DR electrical stimulation evoked dopamine release in the nAcc core. Representative color plot (top) and dopamine concentration trace (bottom) show increase in the release of dopamine in the nAcc core evoked by DR electrical stimulation. Top: Color plot topographically illustrates the voltammetric data with time on the x-axis, applied scan potential (E_{app}) on the y-axis, and background-subtracted faradaic current shown on the z-axis in pseudocolor. Dopamine is identified by an oxidation peak (green) at +0.6 V and a smaller reduction peak (yellow, top) at -0.2 V. Bottom: Corresponding tracer shows the concentration of dopamine (nM) detected in response to electrical stimulation. Onset of the bipolar stimulation was at 5 s with 300 µA, 60 Hz and 120 pulses (red bar). Inset shows characteristic dopamine voltammogram. **C.** Systemic administration of D_2 receptor antagonist eticlopride increases release of dopamine in the nAcc core evoked by DR electrical stimulation. Top: Eticlopride treatment (2 mg/kg, i.p.) increases release of dopamine induced by DR electrical stimulation due to D_2 autoreceptor blockade. Bottom: Corresponding tracer indicates the concentration of dopamine (nM) in response to electrical stimulation after systemic administration of eticlopride. Inset shows characteristic dopamine voltammogram. **D.** The 5-HT reuptake inhibitor fluoxetine does not change dopamine time course evoked by DR electrical stimulation in comparison with eticlopride treatment. Lines indicate dopamine concentrations in the nAcc core after DR electrical stimulation prior to drug treatment (baseline, green line), and after i.p. injection of fluoxetine (10 mg/kg, blue line) or eticlopride (2 mg/kg, pink line). **E.** Systemic administration of the 5-HT_3 receptor antagonist ondansetron significantly decreases dopamine levels evoked by DR stimulation. Bars indicate dopamine concentrations in the nAcc core after DR electrical stimulation prior to drug treatment (baseline, green bar), and after injection of ondansetron (2 mg/kg, i.p., blue bar) or eticlopride (2 mg/kg, i.p., pink bar). The decreasing effect of ondansetron is reversed by systemic administration of eticlopride. Data are shown as mean + s.e.m. (n = 4 each group). A significant difference versus baseline or eticlopride treatment is indicated by ***** or $^{\#}$ (main effect group: $F_{2, 12} = 44.12$, $P = 0.000001$, one-way repeated measures ANOVA; * $P = 0.001$, $^{\#}P = 0.0001$, Newman–Keuls *post-hoc* test). **F.** Dopamine concentration in the nAcc core is decreased by systemic administration of ondansetron. Tracers show the average concentration of dopamine (nM) in the nAcc core after DR stimulation prior to drug treatment (baseline, green line), and after i.p. injection of ondansetron (blue line) or eticlopride (pink line). **G.** A representative surface-plot illustrates changes in dopamine concentration (z-axis), across drug treatment (y-axis) evoked by DR electrical stimulation prior to drug treatment (baseline, green line) and after ondansetron (blue line) or eticlopride (pink line). **H.** Diagram showing microinjection of saline, 5-HT_3 receptor antagonist ondansetron, or AMPA receptor antagonist CNQX into the VTA, and measurement of dopamine release in the nAcc core evoked by DR electrical stimulation. **I.** Disrupting serotonin or glutamate signaling in the VTA reduces dopamine release in the nAcc core evoked by DR electrical stimulation. Intra-VTA microinjection of 5-HT_3 receptor antagonist ondansetron or AMPA receptor antagonist CNQX significantly decreases dopamine release evoked in the nAcc core by DR electrical stimulation. Evoked dopamine release in the nAcc core by DR electrical stimulation prior to drug treatments (baseline, green dashed line), after intra-VTA injection of saline (red bar), ondansetron (3 µg/0.3 µl, blue bar), CNQX (3 µg/0.3 µl, purple bar) or after i.p. injection of eticlopride (2 mg/kg, pink bar). Data are represented as mean + s.e.m. (n = 4 each group). A significant difference versus saline group or eticlopride treatment is indicated by * (main effect group: $F_{3, 12} = 26.11$, $P = 0.00002$, two-way ANOVA; * $P < 0.001$, Newman–Keuls *post-hoc* test, see *P* value in table 2).

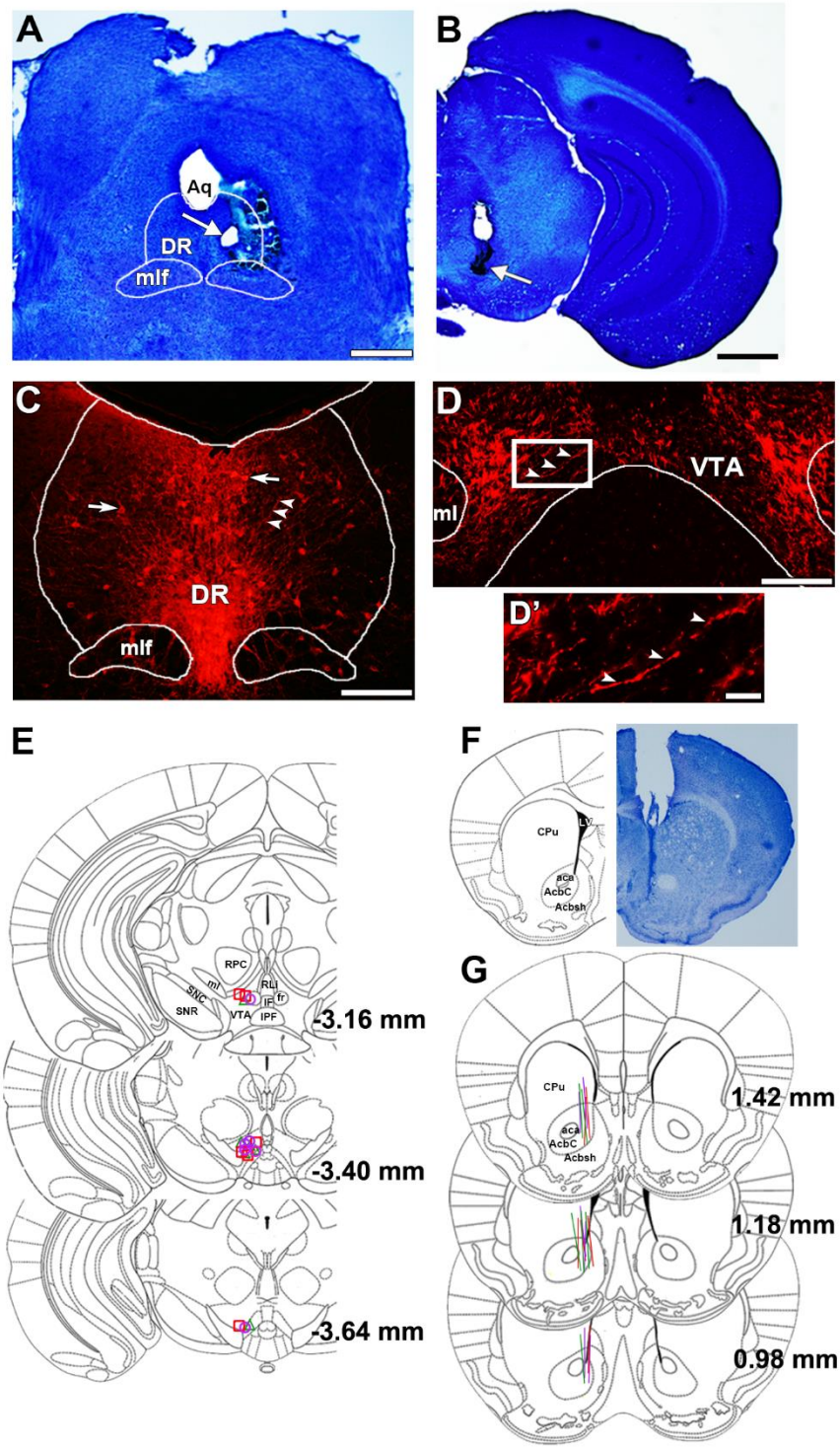

Figure S5. Histological verification of electrode, microinjectors and microdialysis probes placements in wild type mice or SERT::Cre mice. Related to Figure 4.

A. Electrical lesions were used to verify stimulating electrode placements in the DR. Coronal DR sections were stained with cresyl-violet. Arrow points to an example of an electrical lesion hole in the DR. **B.** Histological verification of VTA microinjection site. A representative VTA coronal section is shown as black ink infusion (arrow) into the VTA after microinjections of ondansetron or CNQX. **C-D'.** DR and VTA expression of ChR2-mCherry under the SERT promoter (SERT::Cre mice). Detection of mCherry in the DR (c) and VTA (d,d') of SERT-ChR2-mCherry mice. **C.** mCherry is seen in cell bodies (arrows) and processes (arrowheads). **D,D'**, mCherry is seen in processes within the VTA (arrowheads, closer view in **D'**). Aq, aqueduct; ml, medial lemniscus; mlf, medial longitudinal fasciculus. Scale bars represent 1000 µm in (A and B), 200 µm in (C and D), and 40 µm in (D'). **E.** Microinjector tips in the VTA of SERT-ChR2-eYFP mice are indicated by red squares (ACSF group), green triangles (CNQX group) or purple circles (ondansetron group) in the schematic brain drawings. fr, fasciculus retroflexus; IPF, interpeduncular fossa; ml, medial lemniscus; RLi, rostral liner raphe; RPC, red nucleus parvicellular part; SNC, substantia nigra compacta part; SNR, substantia nigra reticulata part. **F.** Representative microdialysis probe tracks in the nAcc of a SERT-ChR2-eYFP mouse (bregma 1.10 mm). **G.** Microdialysis probes placements in the nAcc are indicated by red (ACSF group), green (CNQX group) or purple (ondansetron) line segments in the schematic brain drawings. aca, anterior commissure anterior part; AcbC, accumbens nucleus core; Acbsh, accumbens nucleus shell; CPu, caudate putamen; LV, lateral ventricle. Diagrams were adapted from mouse atlas.

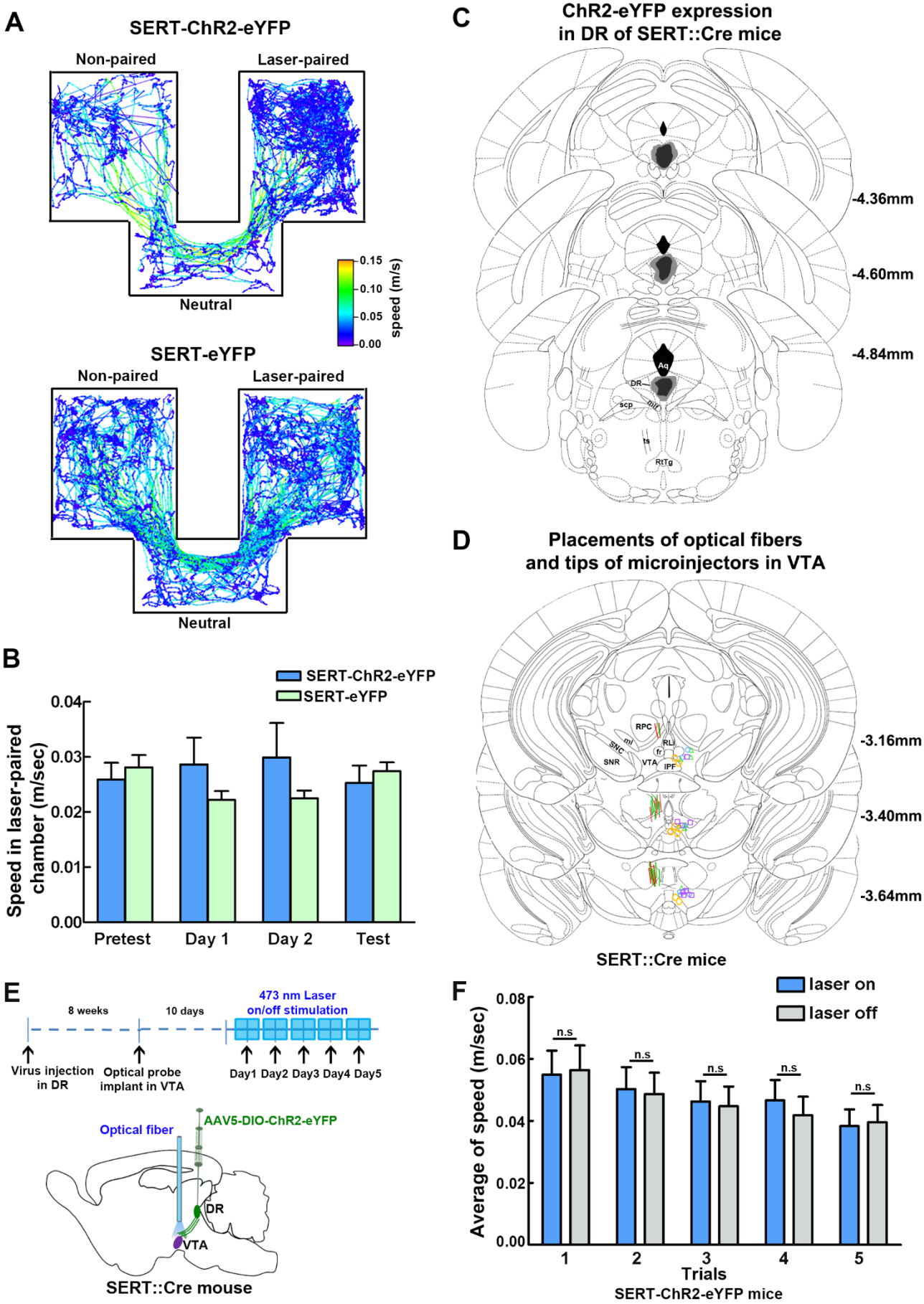
A
SERT-ChR2-eYFP
Non-paired
Laser-paired
Neutral
0.15
0.10
0.05
0.00
speed (m/s)
SERT-eYFP
Non-paired
Laser-paired
Neutral
B
SERT-ChR2-eYFP
SERT-eYFP
Speed in laser-paired chamber (m/sec)
0.04
0.03
0.02
0.01
0.00
Pretest
Day 1
Day 2
Test
C
ChR2-eYFP expression in DR of SERT::Cre mice
-4.36mm
-4.60mm
-4.84mm
Aq
DR
scp
mlf
ts
RtTg
D
Placements of optical fibers and tips of microinjectors in VTA
-3.16mm
-3.40mm
-3.64mm
RPC
SNC
SNR
VTA
RLi
IPF
SERT::Cre mice
E
8 weeks
10 days
473 nm Laser on/off stimulation
Virus injection in DR
Optical probe implant in VTA
Day1 Day2 Day3 Day4 Day5
Optical fiber
AAV5-DIO-ChR2-eYFP
DR
VTA
SERT::Cre mouse
F
laser on
laser off
Average of speed (m/sec)
0.08
0.06
0.04
0.02
0.00
n.s
1
2
3
4
5
Trials
SERT-ChR2-eYFP mice

Figure S6. SERT-ChR2-eYFP mice show preference to the laser-paired chamber. Related to Figure 5.

A. ChR2-eYFP mice spent more time in the laser-paired chamber on test day. Tracking data showing representative traces from a ChR2-eYFP (top) or an eYFP (bottom) mouse on test day. **B.** Laser stimulation does not alter locomotor activity. Bars show the average speed (m/s) for each group of mice in pretest day, laser-paired training days and test day ($F_{1,24}$ =1.34, P = 0.26, SERT-ChR2-eYFP mice versus SERT-eYFP mice). **C.** Maximal (grey) and minimal (black) cellular viral infection within the DR. Coronal sections coordinates are indicated with reference to the mouse atlas. Aq, aqueduct; DR, dorsal raphe; mlf, medial longitudinal fasciculus; RtTg, reticulotegmental nucleus of the pons; scp, superior cerebellar peduncle; ts, tectospinal tract. **D.** Optical fibers placements and tips of microinjectors in VTA. Lines indicate the location of optical fibers within the VTA of SERT-ChR2-eYFP (green) or SERT-eYFP (red) mice. Microinjector tips in VTA of SERT-ChR2-eYFP mice are indicated by green triangles (ACSF group), blue circles (ondansetron group), orange rectangles (ketanserin group) and purple squares (CNQX group). **E.** Diagram showing experiment timeline, virus injection in DR of SERT::Cre mice, and VTA optical activation of DR SERT terminals. **F.** VTA optical activation of DR inputs does not alter locomotor activity of SERT-ChR2-eYFP mice. Mouse locomotor activity were measured daily in an open field chamber in the five trials with and without optical stimulation (two-way ANOVA, optical stimulation effect: $F_{1,9}$ = 1.201, P = 0.302. n = 10). All values are represented as mean + s.e.m. fr, fasciculus retroflexus; IPF, interpeduncular fossa; ml, medial lemniscus; RLi, rostral liner raphe; RPC, red nucleus parvicellular part; SNC, substantia nigra compacta part; SNR, substantia nigra reticulata part.

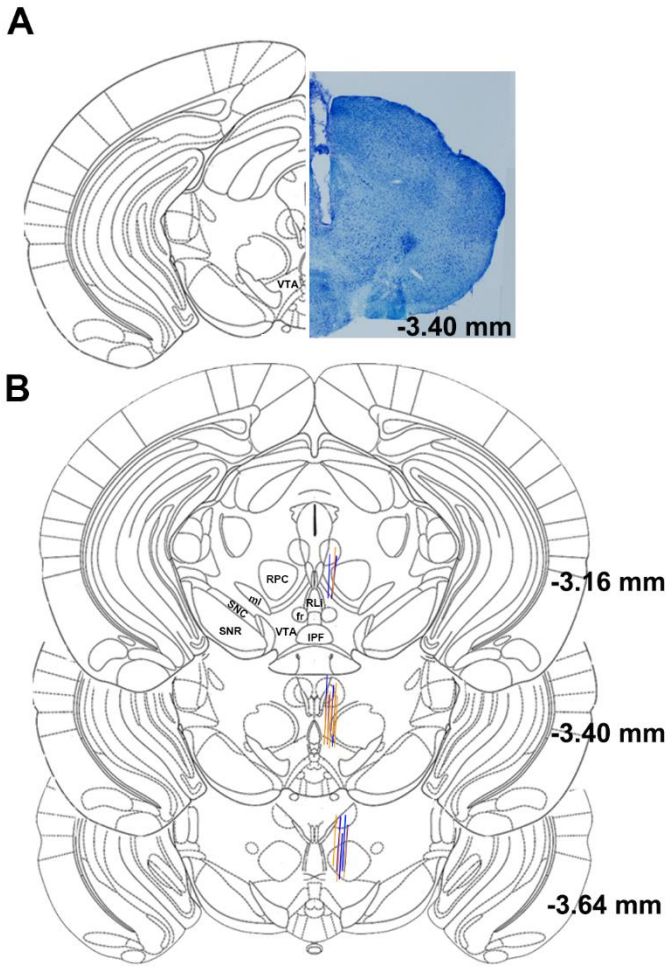

Figure S7. Localization of optical fibers in the VTA of SERT::Cre or VGluT3::Cre mice. Related to Figure 6.

A. Representative optical fiber track in VTA of a SERT-ChR2-eYFP mouse. **B.** Optical fibers placements in the VTA are indicated by blue (VGluT3-ChR2-eYFP mice) or orange (SERT-ChR2-eYFP mice) line segments in the schematic brain drawings. fr, fasciculus retroflexus; IPF, interpeduncular fossa; ml, medial lemniscus; RLi, rostral liner raphe; RPC, red nucleus parvicellular part; SNC, substantia nigra compacta part; SNR, substantia nigra reticulata part.

Table S1. Frequency of TH neurons coexpressing 5-HT$_{3A}$ mRNA in the VTA[a]. Related to Figure 4.

bregma (mm)	subject	Percentage of TH neurons coexpressing 5-HT$_{3A}$ within the total population of 5-HT$_{3A}$ neurons in the VTA	Percentage of TH neurons coexpressing 5-HT$_{3A}$ within the total population of TH neurons in the VTA
-4.92	1	83.9% (*n* = 115)	29.6% (*n* = 115)
	2	83.9% (*n* = 99)	30.8% (*n* = 99)
	3	78.8% (*n* = 108)	30.3% (*n* = 108)
	mean ± s.e.m.	**82.2 ± 1.7% (*n* = 322)**	**30.3 ± 0.4% (*n* = 322)**
-5.40	1	83.3% (*n* = 148)	24.4% (*n* = 148)
	2	83.6% (*n* = 138)	27.5% (*n* = 138)
	3	84.6% (*n* = 181)	28.4% (*n* = 181)
	mean ± s.e.m.	**83.9 ± 0.4% (*n* = 464)**	**26.8 ± 1.2% (*n* = 464)**
-5.88	1	84.5% (*n* = 163)	26.6% (*n* = 163)
	2	84.2% (*n* = 128)	27.9% (*n* = 128)
	3	82.4% (*n* = 131)	26.0% (*n* = 131)
	mean ± s.e.m.	**83.7 ± 0.7% (*n* = 422)**	**26.9 ± 0.6% (*n* = 422)**

[a]TH neurons coexpressing 5-HT$_{3A}$ mRNA were counted in 12 µm thick sections from 3 different rats (subject 1, 2, 3). *n* = total number of TH neurons coexpressing 5-HT$_{3A}$ mRNA in the VTA.

Table S2. *P* value corresponded to each figure.

Figure	*P* value	In comparison with	Statistical method
Figure 4F Time 40 min	0.000037	40 min vs. 20 min	Newman – keuls post hoc test
Figure 4F Time 40 min	0.000038	40 min vs. 30 min	Newman – keuls post hoc test
Figure 4F Time 40 min	0.025966	40 min vs. 50 min	Newman – keuls post hoc test
Figure 4F Time 40 min	0.019750	40 min vs. 60 min	Newman – keuls post hoc test
Figure 4F Time 40 min	0.003285	40 min vs. 70 min	Newman – keuls post hoc test
Figure 4F Time 40 min	0.007488	40 min vs. 80 min	Newman – keuls post hoc test
Figure 6B Sert-ChR2-eYFP	0.0005	Laser-paired vs. non-paired on day 1	Newman – keuls post hoc test
Figure 6B Sert-ChR2-eYFP	0.0006	Laser-paired vs. non-paired on day 2	Newman – keuls post hoc test
Figure 6B Sert-ChR2-eYFP	0.00005	Laser-paired vs. non-paired on test 1	Newman – keuls post hoc test
Figure 6B Sert-ChR2-eYFP	0.00002	Laser-paired vs. non-paired on test 2	Newman – keuls post hoc test
Figure 6B Sert-ChR2-eYFP	0.00099	Laser-paired vs. non-paired on test 3	Newman – keuls post hoc test
Figure 6B Sert-ChR2-eYFP	0.799	Laser-paired vs. non-paired on test 4	Newman – keuls post hoc test
Figure 6B VGluT3-ChR2-eYFP	0.00003	Laser-paired vs. non-paired on day 1	Newman – keuls post hoc test
Figure 6B VGluT3-ChR2-eYFP	0.00004	Laser-paired vs. non-paired on day 2	Newman – keuls post hoc test
Figure 6B VGluT3-ChR2-eYFP	0.00002	Laser-paired vs. non-paired on test 1	Newman – keuls post hoc test
Figure 6B VGluT3-ChR2-eYFP	0.00005	Laser-paired vs. non-paired on test 2	Newman – keuls post hoc test
Figure 6B VGluT3-ChR2-eYFP	0.491	Laser-paired vs. non-paired on test 3	Newman – keuls post hoc test
Figure 6B VGluT3-ChR2-eYFP	0.931	Laser-paired vs. non-paired on test 4	Newman – keuls post hoc test
Figure 3I	0.00402	1.5 s vs. baseline	Newman – keuls post hoc test
Figure 3I	0.00010	2.5 s vs. baseline	Newman – keuls post hoc test
Figure 3I	0.00221	3.5 s vs. baseline	Newman – keuls post hoc test
Figure 3I	0.00062	4.5 s vs. baseline	Newman – keuls post hoc test
Figure 3I	0.00004	5.5 s vs. baseline	Newman – keuls post hoc test
Figure 3I	0.01470	6.5 s vs. baseline	Newman – keuls post hoc test
Figure 3J	0.00005116	1.5 s vs. baseline	Newman – keuls post hoc test
Figure 3J	0.00001685	2.5 s vs. baseline	Newman – keuls post hoc test
Figure 3J	0.00001593	3.5 s vs. baseline	Newman – keuls post hoc test
Figure 3J	0.00005513	4.5 s vs. baseline	Newman – keuls post hoc test
Figure 3J	0.00004830	5.5 s vs. baseline	Newman – keuls post hoc test
Figure 3J	0.00006257	6.5 s vs. baseline	Newman – keuls post hoc test
SupplementaryFigure 4I	0.01	Ondansetron vs. saline	Newman – keuls post hoc test
Supplementary Figure 4I	0.04	CNQX vs. saline	Newman – keuls post hoc test
Supplementary Figure 4I	0.0002	Ondansetron vs. eticlopride	Newman – keuls post hoc test
Supplementary Figure 4I	0.0002	CNQX vs. eticlopride	Newman – keuls post hoc test